








Research Article

Postprocessing of MRIs Using FreeSurfer in Epilepsy Surgery Patients Provides an Excellent Imaging Marker of Hippocampal Sclerosis but Fails to Separate Subtypes

Ane G. Kloster ¹, Giske Opheim,¹ Kristin Å. Alfstad ², Karen B. Larsen,^{3,4} Pitt Niehusmann,⁵ Emil Holm,¹ Philip Fink-Jensen,¹ Eva Løbner Lund ^{3,4}, Bo Jespersen,⁶ Jugoslav Ivanovic,⁷ Guido Rubboli ^{3,8}, Camilla G. Madsen,⁹ Pål B. Marthinsen ¹⁰, Melanie Ganz ^{1,11}, Morten Lossius,^{2,12} and Lars H. Pinborg ^{1,3,13}

¹Neurobiology Research Unit, Copenhagen University Hospital-Rigshospitalet, Copenhagen, Denmark

²National Centre for Epilepsy, Oslo University Hospital, Norway

³Faculty of Health and Medical Sciences, University of Copenhagen, Denmark

⁴Department of Pathology, Copenhagen University Hospital-Rigshospitalet, Denmark

⁵Department of Pathology, Oslo University Hospital-Rikshospitalet, Norway

⁶Department of Neurosurgery, Copenhagen University Hospital-Rigshospitalet, Denmark

⁷Department of Neurosurgery, Oslo University Hospital-Rikshospitalet, Norway

⁸Danish Epilepsy Centre, Dianalund, Denmark

⁹Functional and Diagnostic Imaging Unit, Department of Radiology, Copenhagen University Hospital - Hvidovre, Denmark

¹⁰Department of Radiology, Oslo University Hospital-Rikshospitalet, Norway

¹¹Department of Computer Science, University of Copenhagen, Denmark

¹²Institute of Clinical Medicine, University of Oslo, Norway

¹³Epilepsy Clinic, Department of Neurology, Copenhagen University Hospital-Rigshospitalet, Denmark

Correspondence should be addressed to Lars H. Pinborg; lars.pinborg@nru.dk

Received 2 September 2022; Revised 29 January 2023; Accepted 10 April 2023; Published 24 May 2023

Academic Editor: Dominic B. Fee

Copyright © 2023 Ane G. Kloster et al. This is an open access article distributed under the Creative Commons Attribution License, which permits unrestricted use, distribution, and reproduction in any medium, provided the original work is properly cited.

Objective. Histopathological examinations will diminish as minimally invasive epilepsy surgery increasingly replaces open surgery. The objective of this study was to test if visual and computer-aided quantitative analyses of presurgical high-quality 3 Tesla MRIs complying with the International League Against Epilepsy (ILAE) Neuroimaging Task Force recommendations can inform on histopathological diagnosis. **Methods.** Ninety-two patients from Copenhagen and Oslo University Hospitals fulfilled patient-, imaging-, and histopathological inclusion criteria: 69 patients were diagnosed with hippocampal sclerosis (HS) ILAE type 1 or 2, and 23 patients had normal appearing hippocampi or other histopathology than HS (no-HS). MRIs from 52 healthy controls (HC) were included. Image processing was performed in *FreeSurfer v.6.0* with the built-in cross-sectional hippocampal subfield segmentation tool and multimodal MRI input. Volume outputs were used to calculate volume asymmetry ratios (VARs) for whole hippocampus (WH) and subfields. **Results.** HS patients had significantly larger WH VARs compared to no-HS patients and HC, with a sensitivity = 0.93 and specificity = 1.0 for histopathological HS diagnosis. Visual MRI assessment yielded a sensitivity = 0.90 and specificity = 0.96 for histopathological HS diagnosis. CA1 and CA4 VARs and the number of seizure-free patients were not significantly different in HS ILAE type 1 compared to type 2 patients. **Significance.** FreeSurfer analyses of presurgical MRIs are excellent at separating patients histopathologically diagnosed with HS from patients with other pathology or normal appearing hippocampi. Using the FreeSurfer hippocampal subfield segmentation tool did not allow for separating HS ILAE subtypes.

1. Introduction

In 2019, the International League Against Epilepsy (ILAE) Neuroimaging Task Force recommended the use of the Harmonized Neuroimaging of Epilepsy Structural Sequences Magnetic Resonance Imaging (HARNES-MRI) protocol with isotropic, millimetric 3D T1-weighted (T1w) and fluid-attenuated inversion recovery (FLAIR) images and high-resolution 2D submillimetric T2-weighted (T2w) images for best-practice neuroimaging of epilepsy patients [1]. The Task Force endorsed the use of computer-aided image postprocessing methods to provide an objective account of an individual's brain anatomy and pathology [1].

Hippocampal sclerosis (HS) is the archetypal abnormality found in temporal lobe epilepsy (TLE) patients [2]. HS patients are frequently drug-resistant [3–5] and may be eligible for surgical intervention with seizure freedom rates ranging between 53 and 84% one year after surgery [6, 7]. HS is histopathologically characterized by segmental loss of pyramidal neuronal cells and increased gliosis (i.e., sclerosis) of the hippocampus. In 2013, the ILAE Commission on Diagnostic Methods [8] introduced a new semiquantitative classification system for HS, depending on the specific pattern of neuronal cell loss within the four different subfields of the hippocampal cornu ammonis (CA) [8]. HS ILAE type 1 is characterized by severe neuronal cell loss in both CA1 and CA4 subfields, while HS ILAE type 2 and type 3 predominantly portray neuronal loss in CA1 or CA4 subfield, respectively. The aim of the classification was to establish a single and reproducible system across centers that differentiates histopathologic subgroups and their relation to postsurgical outcomes and comorbidities [8–11]. HS ILAE type 1 has been found to associate with better postsurgical seizure outcomes [8, 9] and memory performance [10, 11] than HS ILAE types 2 and 3. But, the clinical use of HS ILAE classification as a biomarker of postsurgical seizure outcome is limited by its post hoc histopathological confirmation.

HS is diagnosed with high accuracy in MRI by reduced hippocampal volume, obscuration of normal internal architecture, and increased T2w or FLAIR signal intensity on visual examination [1, 8, 12] or by reduced whole-hippocampal volumetry [1, 13–19]. However, identification of subfield-specific atrophy for HS ILAE classification is not feasible by visual examination [8]. Manual delineation of hippocampal subfields has found a good correlation to neuronal density [14, 20] but is time-consuming and difficult to implement in a clinical setting. The development and optimization of computer-aided methods for hippocampal subfield segmentation represent an alternative approach for presurgical volumetry of both whole hippocampus and subfields [1, 21, 22]. The studies on computer-aided subfield segmentation for HS ILAE classification with histopathological correlates available have shown conflicting results: Menzler et al. [23], Riederer et al. [24], and Peixoto-Santos et al. [20] used high-field 3 Tesla (3T) or 1.5 Tesla (1.5T) T1w MRIs and the updated FreeSurfer version 6.0 hippocampal subfield segmentation tool and found good agreement of computer-aided subfield volume reduction and subfield neuronal loss in HS ILAE type 1, but not in type 2

[20, 23, 24] or 3 [23, 24]. The number of patients was small ($n \leq 28$), and high-resolution multimodal input for optimal performance of hippocampal segmentation was not used [19, 22]. Mizutani et al. [25] applied multimodal input and the Automatic Segmentation of Hippocampal Subfield tool but found no correlation between hippocampal subfield volumes and subfield neuronal densities in 24 patients.

In this study, we analyzed the findings of 92 surgically treated and histopathologically diagnosed TLE patients from Denmark and Norway and compared them to 52 healthy controls. We used high-quality 3T T1w and T2w MRIs similar to the proposed HARNES-MRI protocol, the updated hippocampal subfield segmentation tool [22] in FreeSurfer version 6.0 [21], and a simple volume asymmetry ratio (VAR) to test if the presurgical MRI scan is an accurate biomarker (i) for separating HS from other pathologies or normal appearing hippocampal tissue, (ii) for HS ILAE classification, and (iii) for predicting seizure outcome one year after surgery.

2. Methods

2.1. Patients. In this retrospective two-center study, we identified 354 consecutive surgically treated TLE patients at Copenhagen University Hospital-Rigshospitalet in Denmark ($n = 255$) operated between 2009 and 2020 and Oslo University Hospital Rikshospitalet in Norway ($n = 99$) operated between 2012 and 2018. These epilepsy surgery centers conduct all epilepsy surgery procedures in the respective countries and thus represent whole population cohorts. The study was approved by the Danish Protection Agency and the Danish Patient Safety Authority (case numbers 3-3013-1030/1 and 3-3013-3074/1), the Norwegian Regional Committees for Medical and Health Research Ethics (case number 64559), and the Data Protection Office of Oslo University Hospital (case number 20/01450). Parts of the Danish patient material was included in the PhD thesis by coauthor Opheim [26].

In the Norwegian cohort, one patient declined to participate in the study. Preoperative MRIs could not be retrieved in the picture archiving and communication system (PACS) for 34 patients from the Danish cohort operated between 2009 and 2013. To ensure the quality and consistency in the dataset, all patients' MRI sequences were carefully evaluated under the criteria listed in Table 1. A full overview of the patient inclusion and exclusion process is shown in Figure 1, resulting in 92 included TLE patients. They underwent either anteromedial temporal lobectomy ($n = 91$) or selective amygdalohippocampectomy ($n = 1$) and were divided into two groups according to histopathological diagnosis: HS ($n = 69$) or no-HS ($n = 23$) (Figure 1). The HS patients were subdivided according to the ILAE classification for hippocampal sclerosis [8]. No patients were classified as HS ILAE type 3, resulting in the following patient groups: HS ILAE type 1 ($n = 64$), HS ILAE type 2 ($n = 5$), and no-HS ($n = 23$). The no-HS patient group is a histopathologically heterogeneous group. It consists of patients without any histopathological signs of HS and includes TLE patients with tumors or focal cortical dysplasia (FCD) within or outside

TABLE 1: Patient MRI inclusion and exclusion criteria. Details on the individual MRI acquisition parameters are available in supplementary information.

MRI inclusion and exclusion criteria
Inclusion criteria
(i) Presurgical 3 T MRIs from Copenhagen University Hospital Hvidovre or Oslo University Hospital Rikshospitalet including the following sequences:
(a) 3D MPRAGE T1w images with isotropic millimetric voxel resolution
(b) 2D TSE T2w coronal images with high in-plane submillimetric voxel resolution
Exclusion criteria
(i) MRI abnormalities hampering successful processing in FreeSurfer, entailing:
(a) Structural nonepileptogenic lesions (i.e., not presumed to be part of seizure generation or propagation)
(b) Previous brain surgery
(c) Marked movement artefacts

MRI = magnetic resonance imaging; 3 T = 3 Tesla; MPRAGE = magnetization-prepared rapid acquisition gradient echo; T1w = T1-weighted; FSE = fast spin-echo; T2w = T2-weighted.

the hippocampus ($n = 6$) and patients with unspecific reactive gliosis or without any pathologic findings in the hippocampus, amygdala, or temporal neocortex ($n = 17$) (Figure 1).

2.2. Healthy Controls. From the Center for Integrated Molecular Brain Imaging (CIMBI) database [27], we identified 59 healthy controls (HC) meeting the MRI requirements with 3 T 3D T1w and T2w sequences without structural abnormalities or movement artefacts. After processing in FreeSurfer, seven subjects had significant segmentation errors and were excluded. This resulted in a group of 52 HC for group comparisons.

2.3. Histopathology. The surgical specimens were fixated in 10% buffered formalin for 12-24 hours. After macroscopic examination, the tissue was sectioned into 4 mm interval parallel slices according to coronal planes along an anterior-posterior axis. Tissue blocks were postfixed, transferred to 10% buffered formalin, dehydrated, and embedded in paraffin wax. Sections were stained with hematoxylin and eosin or used for immunohistochemistry (NeuN, neuronal marker). The reagents used for immunostaining came from EnVision™ FLEX+ High pH kit (K8012), Dako. Antigen retrieval was carried out at pH9 for 20 minutes with a PT link module. Staining was done according to manufacture instructions: sections were incubated with peroxidase for 5 minutes, mouse linker (K8022) for 15 minutes, and then anti-NeuN (1:800, Millipore, MAB377) for 20 minutes. Antibody binding visualization was performed by incubation with a labelled HRP polymer for 20 minutes and a signal as generated with a 3,3'-diaminobenzidine-tetrahydrochloride (DAB chromogen) for 10 minutes. Hematoxylin was used for counterstaining. To ensure correct HS ILAE classification across countries, consensus understanding of the classification was discussed beforehand and verified by

direct contact with the first author of the HS ILAE consensus article Dr. I. Blümcke [8]. All specimens were examined by neuropathologists specialized in evaluating epilepsy surgery tissue, blinded to the volumetry results. All HS specimens were reexamined to ensure correct ILAE classification. Specimens with uncertain findings were discussed among colleagues, and if consensus on classification was not possible, the cases were labeled "no HS subclassification" and excluded from the study (13 of 82 HS patients, 16%, Figure 1).

2.4. MRI Scan Protocol. Danish patients and healthy controls were imaged at Copenhagen University Hospital, Hvidovre, using Siemens Healthcare Magnetom Verio (patients, $n = 73$) and Magnetom Trio (healthy controls, $n = 52$) 3 T MRI systems with 32- and eight-channel head coils, respectively. Norwegian patients were imaged at Oslo University Hospital, Rikshospitalet, using Siemens Healthcare Magnetom Skyra ($n = 17$) or Philips Healthcare Achieva ($n = 2$) 3 T MRI systems with a 32-channel or eight-channel head coil, respectively. Specifications of the applied MRI sequences are listed in Table 1. More details on the MRI acquisition parameters are available in the supplementary information (available here).

2.5. Neuroradiological Visual Assessment. All patients' MRIs were routinely visually examined and diagnosed upon acquisition and then reassessed by neuroradiologists trained at detecting epileptogenic lesions as part of the presurgical evaluation of epilepsy patients. The neuroradiologists were blinded to both histopathology and volumetric analyses.

2.6. Postsurgical Seizure Outcome. The seizure outcomes were assessed for all patients one year following surgery. The patients were classified according to the ILAE outcome score [28] into seizure-free (ILAE class 1) and non-seizure-free (ILAE classes 2-6).

2.7. Data Analysis. Image processing was performed in *FreeSurfer version 6.0* [21], with the built-in cross-sectional hippocampal subfield segmentation tool [22]. All hippocampal segmentations were performed with the multimodal option of adding T2w images as overlays to the T1w images to increase boundary tracing accuracy in the outer hippocampi as well as in the subfields. The hippocampal subfield segmentation outputs from both Copenhagen and Oslo were visually quality assessed by the same experienced observer. Left and right hippocampal volumes (whole hippocampus (WH), CA1, and CA4) were exported for statistical analysis.

2.8. Statistical Analysis. In MATLAB (R2021a), VARs were calculated for each hippocampal region (WH, CA1, and CA4). For patients, the volume ipsilateral to the surgical site was subtracted from the contralateral volume and divided by the sum of both volumes. The healthy controls were randomized into left and right, subtracting one side from the other, dividing by the sum of both volumes. Using within-subject VARs eliminates the need to correct for intracranial volumes (ICV) and allows for pooling of right- and left-sided TLE patients. In MATLAB, violin plots were generated using the *bastibe* function [29] and receiver operating

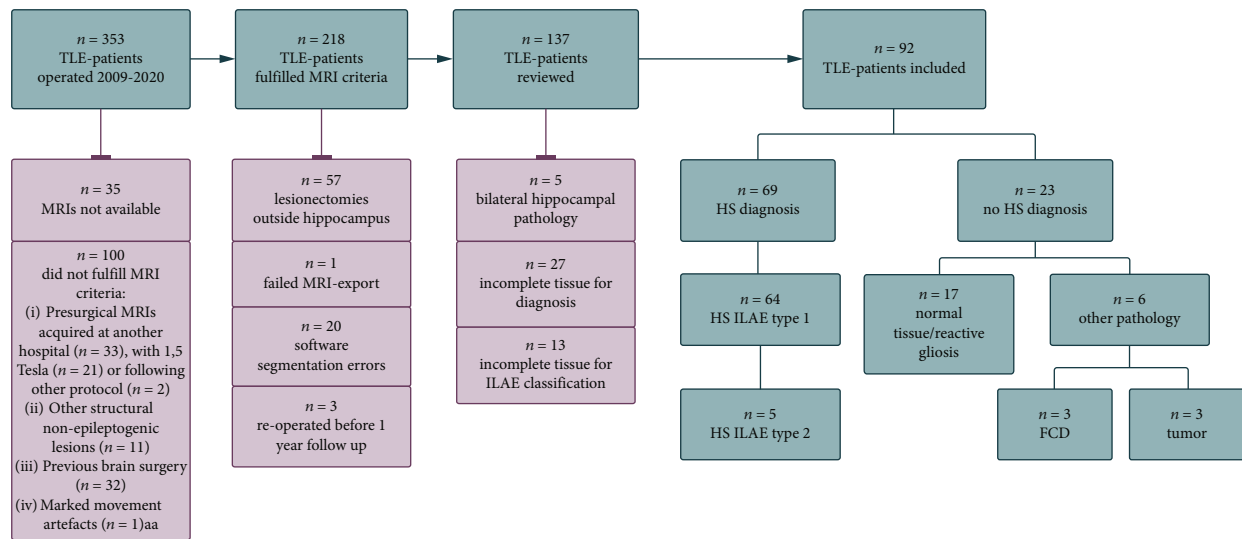


FIGURE 1: Overview of excluded and included TLE patients. The flow chart shows the patient inclusion process where excluded patients are marked in red and represent patients that (i) did not have presurgical MRIs available for export, (ii) did not meet the MRI criteria listed in Table 1, (iii) had lesionectomies where the hippocampus was not included in the resection, (iv) MRIs that could not be exported, (v) had clinically significant software segmentation errors in FreeSurfer, (vi) were reoperated before one year postsurgical follow-up, (vii) had bilateral hippocampal pathology, or (viii) had incomplete or fragmented hippocampal tissue samples that were insufficient for histopathological diagnosis or HS ILAE classification. The resulting 92 included TLE patients are presented according to histopathological diagnosis. TLE = temporal lobe epilepsy; MRI = magnetic resonance imaging; HS = hippocampal sclerosis; ILAE = International League Against Epilepsy; FCD = focal cortical dysplasia.

characteristic (ROC) curves using the built-in `perfcurve` function. Statistical testing at group level was performed in R (R Core Team 2021) using the two-tailed Wilcoxon Mann–Whitney (WMW) rank-sum test from the `asht` package. p values were calculated by asymptotic method or by exact method with complete enumeration or the Monte Carlo implementation in comparisons where the small HS ILAE type 2 patient group ($n = 5$) was included. All p values were corrected for multiple comparison ad modum Bonferroni ($p_{\text{corrected}} = (p_{\text{uncorrected}} \times 8 \text{ comparisons} \times 3 \text{ regions})$). From the `asht` package, effect sizes (WMW estimates) were calculated for each comparison, expressing the probability that the VAR of a randomly selected subject from one group is larger than the VAR of a randomly selected subject from another group. Student's t -test and chi-square or Fischer's exact test were used for testing demographic and seizure outcome group differences for continuous and categorical variables, respectively.

3. Results

In Figure 2, VARs of patients and healthy controls are graphically depicted as a violin plot. It demonstrates the significantly larger VAR values found throughout all regions in HS patients compared to the no-HS patients and healthy controls (Table 2). Figure 3(a) shows a bootstrapped ($n = 1000$) ROC curve for detection of HS based on WH and CA1 VARs in the HS patient group versus the no-HS patient group. ROC curve analysis yielded an AUC_{WH} of 0.98 with a sensitivity of 0.93 and specificity of 1.0 at the optimal cutoff for diagnosis ($\text{VAR}_{\text{WH}} \geq 0.06$). AUC_{CA1} was

also 0.98, with sensitivity of 0.97 and specificity of 0.91 at the optimal cutoff for diagnosis ($\text{VAR}_{\text{CA1}} \geq 0.04$).

Figure 3(b) shows the contingency table for HS diagnosis by neuroradiological visual assessment, with a sensitivity of 0.90 and specificity of 0.96. One of 23 no-HS patients (4%) was misdiagnosed with HS by the neuroradiologist but correctly diagnosed by the computer-aided WH VAR approach. Seven of 69 HS patients (10%) were not diagnosed with HS by neuroradiological visual examination, whereas the computer-aided VAR approach correctly identified the patients as having HS in five of seven cases. In three of these seven cases, the neuroradiologists described possible but not decisive signs of HS. Reversely, the computer-aided VAR approach did not misdiagnose any no-HS patients as having HS but failed to diagnose HS in five of 69 HS patients (7%). Three of these five were correctly diagnosed with HS by visual examination (one solely on increased signal intensity). The combined performance of HS diagnosis by the computer-aided VAR approach and visual assessment yielded a sensitivity and specificity of 0.97 and 1.0, respectively.

Statistical testing of groups with the WMW rank-sum test showed significantly increased VAR in WH, CA1, and CA4 for both HS ILAE type 1 and type 2 compared to healthy controls and the no-HS patient group, with large effect size measures (≥ 0.96) (see p values and effect sizes in Table 2). The WMW effect size estimates for WH and CA1 VAR differences between the HS and no-HS patient groups were equal to the AUCs of the ROC curve (0.98). There were no significant VAR differences in WH, CA1, and CA4 when comparing HS ILAE type 1 with type 2, effect sizes 0.34–0.57. There were no significant VAR differences between the no-HS patient group and healthy controls, effect sizes 0.36–0.41.

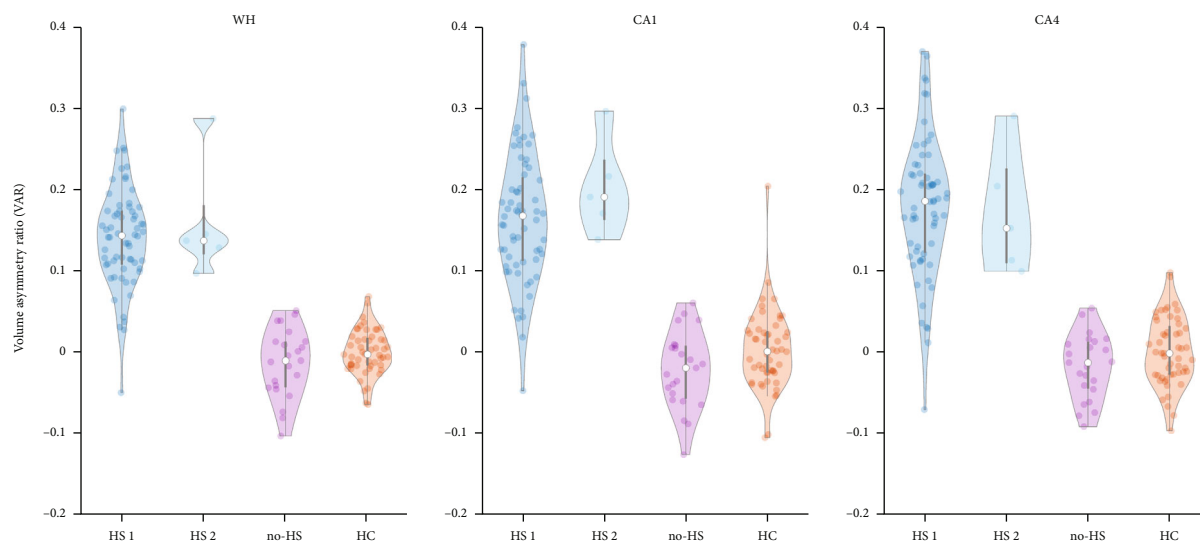


FIGURE 2: Violin plot displaying distributions of volume asymmetry ratios with overlaying data points in all four groups across the four hippocampal regions. For each of the three hippocampal regions (WH, CA1, and CA4), the distribution of volume asymmetry ratios for each patient group and the healthy controls is represented by a violin shape. The shape outline represents a kernel density estimate of the data for each group with overlaying data points. Within the center of each violin, the white dot represents the median value, and the grey line represents the 25th and 75th percentiles. HS = hippocampal sclerosis; HC = healthy controls; Std = standard deviations; WH = whole hippocampus; CA = cornu ammonis; ILAE = International League Against Epilepsy.

TABLE 2: Results of group comparisons using the Wilcoxon Mann–Whitney rank-sum test. For every group comparison, p values corrected for multiple comparison ($p_{\text{corrected}} = (p_{\text{uncorrected}} \times 8 \text{ comparisons} \times 3 \text{ regions})$) are listed within each region (WH, CA1, and CA4).

	WH		CA1		CA4	
	Effect size	p values	Effect size	p values	Effect size	p values
HS ILAE 1 vs. no-HS	0.98	3.28×10^{-10}	0.98	2.05×10^{-10}	0.98	3.07×10^{-10}
HS ILAE 1 vs. HC	0.98	2.52×10^{-17}	0.96	5.41×10^{-16}	0.96	2.28×10^{-16}
HS ILAE 2 vs. no-HS	1.00	4.88×10^{-4}	1.00	4.88×10^{-4}	1.0	4.88×10^{-4}
HS ILAE 2 vs. HC	1.00	4.80×10^{-3}	0.99	4.80×10^{-3}	1.0	4.80×10^{-3}
HS ILAE 1 vs. HS ILAE 2	0.49	1.00	0.34	1.00	0.57	1.00
No-HS vs. HC	0.41	1.00	0.36	1.00	0.39	1.00
HS vs. no-HS	0.98	1.74×10^{-10}	0.98	1.11×10^{-10}	0.98	1.63×10^{-10}
HS vs. HC	0.98	5.03×10^{-18}	0.96	1.11×10^{-16}	0.97	4.19×10^{-17}

Significant values ($p < 0.05$) are presented in bold. Effect sizes are derived from the Wilcoxon Mann–Whitney (WMW) estimate from the `asht` package in R, estimating the probability that the VAR of a randomly selected subject from the group listed to the left of the comparison is larger than the VAR of a randomly selected subject from the group to the right. HS = hippocampal sclerosis; ILAE = International League Against Epilepsy; HC = healthy controls; WH = whole hippocampus; CA = cornu ammonis.

In the HS patient group, 43 of 69 patients (62%) were seizure-free one year following surgery, compared to 15 of 23 (65%) in the no-HS patient group, with no significant difference between the two groups ($\chi^2(1, n = 92) = 0.062$, $p = 0.80$). There was no significant difference in the number of seizure-free HS ILAE type 1 (39 of 64, 61%) and type 2 (4 of 5, 80%) patients ($p = 0.64$, Fisher's exact test). We found no difference in WH or subfield VARs of seizure-free HS patients (43 of 69, 62%) versus non-seizure-free HS patients (26 of 69, 38%) ($p \geq 0.65$, WMW rank-sum test). ROC curve of WH VAR in seizure-free versus non-seizure-free HS patients showed no differentiating ability of the WH VAR in predicting seizure outcome, with an AUC of 0.53.

Demographic data of patients and controls are presented in Table 3. There was a significant difference in mean age between patients and healthy controls ($p = 0.00049$, Student's t -test). Age was not correlated to WH VAR using linear regression ($R^2 = 0.000060 - 0.021$, $p = 0.17 - 0.96$). There was no significant difference in gender between patients and controls ($\chi^2(1, n = 144) = 0.22$, $p = 0.64$). Years with epilepsy ($p = 0.00008$, Student's t -test) and years with drug resistance ($p = 0.02$, Student's t -test) were both significantly longer in HS patients compared to the no-HS patients. In HS ILAE type 1 and type 2 patients, there was no significant difference in years with epilepsy ($p = 0.11$, Student's t -test) or years with drug resistance ($p = 0.74$, Student's t -test).

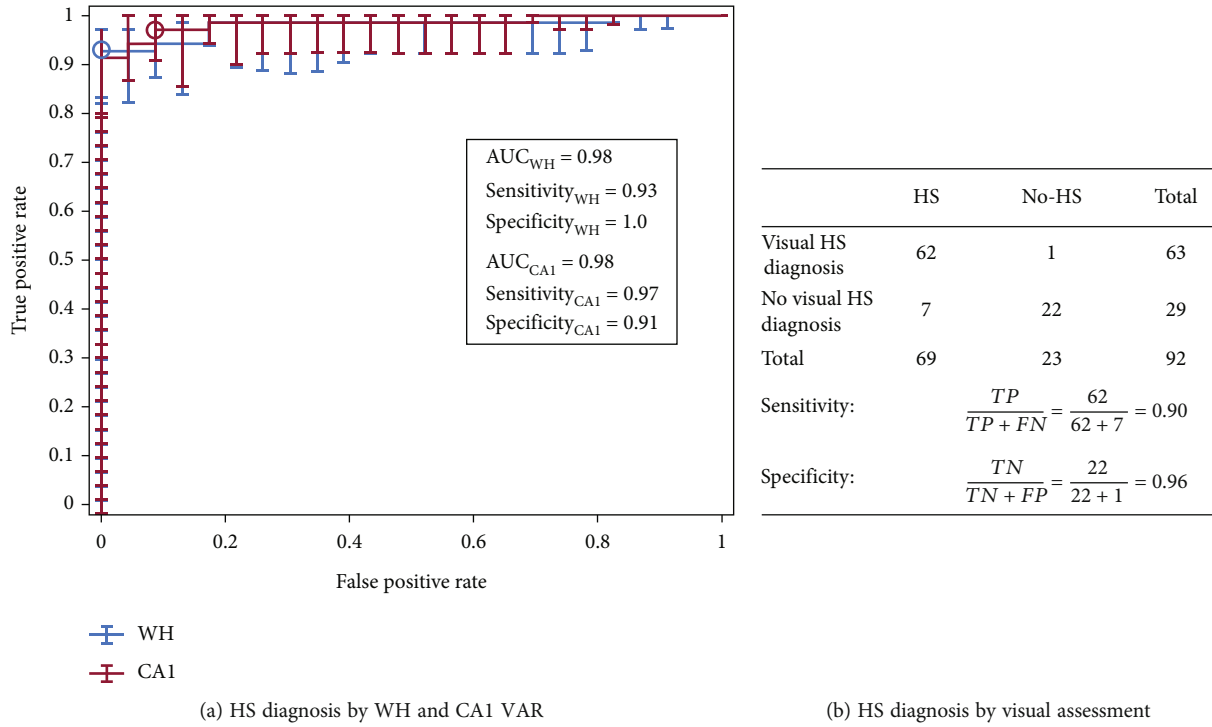


FIGURE 3: HS diagnosis by computer-aided method (a) and expert visual assessment (b). (a) The bootstrapped ($n = 1000$) receiver operator characteristic (ROC) curve for detection of HS based on WH and CA1 volume asymmetry ratios (VARs) in the HS patient group versus the no-HS patient group. For each data point, the brackets represent the bootstrap-generated confidence interval for the curve. The text box lists the area under the curve (AUC) values and the sensitivity, specificity, and VAR values at the optimal threshold of the curve (blue and red circles). (b) The contingency table for HS diagnosis by visual examination performed by neuroradiologists specialized in epilepsy diagnostics. HS = hippocampal sclerosis; WH = whole hippocampus; TP = true positives; FP = false positives; TN = true negatives; FN = false negatives.

TABLE 3: Demographic characteristics of patients and controls.

	Healthy controls ($N = 52$)	HS patients		No-HS ($N = 23$)
		HS ILAE 1 ($N = 64$)	HS ILAE 2 ($N = 5$)	
Sex				
Female	25 (48%)	36 (56%)	4 (80%)	8 (35%)
Male	27 (52%)	28 (44%)	1 (20%)	15 (65%)
Age (years)				
Mean (SD)	48 (± 21)	36 (± 17)	43 (± 12)	35 (± 13)
Years with epilepsy				
Mean (SD)		21 (± 16)	36 (± 16)	11 (± 8.2)
Years with drug resistance				
Mean (SD)		17 (± 14)	19 (± 16)	11 (± 8.4)
Laterality				
Left	26 (50%)	37 (58%)	1 (20%)	16 (70%)
Right	26 (50%)	27 (42%)	4 (80%)	7 (30%)
Outcome				
Non-seizure-free		25 (39%)	1 (20%)	8 (35%)
Seizure-free		39 (61%)	4 (80%)	15 (65%)

Years with epilepsy: years from diagnosis of epilepsy to surgery. *Duration drug-resistant*: years of drug-resistant epilepsy (i.e., failure of adequate trials of two appropriately chosen and used antiepileptic drug schedules [45]). *Laterality*: side of operation (patients) or randomized (HC). *Outcome*: seizure outcome one year after surgery according to the ILAE outcome score [28], where seizure-free patients have a score of 1 (completely seizure-free) and the non-seizure-free patients have any form of seizures with scores 2-5 (from auras only to an increase in baseline seizure days). Categorical values are presented with frequencies and percentages and continuous values with means and standard deviations (SD).

4. Discussions

4.1. Presurgical MRI as a Biomarker for Diagnosing HS. In this study, we demonstrate that combining a presurgical high-quality T1w and T2w 3 T MRI protocol, the updated hippocampal subfield segmentation tool implemented in FreeSurfer v. 6.0, and a simple VAR is an excellent biomarker for separating patients histopathologically diagnosed with HS from patients with other pathology or normal appearing hippocampi.

The violin plot in Figure 2 clearly shows the VAR differences between TLE patients with and without HS. The ability of both WH and CA1 VAR to diagnose HS among TLE patients is demonstrated in the ROC plot in Figure 3(a) with excellent AUC values of 0.98 and remarkably high sensitivities and specificities > 0.9 at VAR thresholds of 0.06 and 0.04, respectively. Reduced WH volume is a recognized MRI surrogate marker for HS [1, 13–18]. Even though CA1 makes up almost 50% of the total hippocampal volume [20] and is specifically affected in both HS ILAE type 1 and 2 [8], CA1 VAR did not diagnose HS with greater specificity compared to the WH VAR. This may be due to a ceiling effect related to the excellent AUC values of both approaches. Compared to previous studies, we find the highest accuracy for a computer-aided HS diagnosis [15, 16, 30]. Our study is unique in combining very strict patient and imaging criteria for inclusion of patients, a large sample of epilepsy surgery patients, the use of the newest FreeSurfer segmentation tool and comparing operated patients with a histopathologically verified HS diagnosis to patients with a no-HS diagnosis.

We demonstrated that the ability to separate HS patients from no-HS patients by quantitative hippocampal assessment using FreeSurfer is very similar to visual MRI assessment by experienced neuroradiologists in the epilepsy surgery teams (Figure 3) and that combining the visual and computer-aided assessment further improved the sensitivity and specificity to 0.97 and 1.0, respectively. This observation is of clinical significance particularly looking into a future where minimal invasive surgery techniques [31–33] will preclude histopathological examination and presurgical MRI will be increasingly important as a biomarker for histopathology. But the patients to benefit the most from introducing the HARNESS-MRI protocol and computer-aided image postprocessing methods are most likely patients newly diagnosed with epilepsy, where MRI lesions may be subtle and easily overlooked [1, 18, 30]. The early identification of HS is of importance for clinicians to inform patients on best possible epilepsy treatment and mitigate the potential consequences of drug resistance [4, 34] and thence cognitive decline, psychiatric disease, and reduced quality of life [5, 35].

4.2. Presurgical MRI as a Biomarker for HS ILAE Classification. Contrary to what we expected, we found no significant difference in CA4 VARs in patients histopathologically classified as HS ILAE type 1 compared to HS ILAE type 2 ($p = 1.0$, Table 2), and the CA4 VARs were significantly larger in both HS ILAE type 1 and 2 patients compared to no-HS patients and healthy controls ($p < 0.005$)

(Table 2 and Figure 2). The statistical power of our analysis is challenged by the fact that only five patients were histopathologically classified with HS ILAE type 2, but we expect that a computer-aided VAR approach for differentiating ILAE subtypes must provide robust results in individual patients to be feasible in a clinical setting.

Peixoto-Santos et al. [20] is the only other study to test computer-aided subfield volumes of different histopathological HS ILAE types against each other, reporting no subfield VAR differences between HS ILAE types 1 ($n = 22$) and 2 ($n = 6$). Notably, they performed subfield volumetry by manual segmentation in the same HS ILAE type 2 patients, finding intact CA4 subfield volumes and reduced subfield volume only in CA1, in accordance with the histopathological neuronal cell loss. Their findings are corroborated by previous studies showing good correlation between manual subfield volumetry and ILAE classification [1, 8, 14, 20]. The discrepancy between manual and computer-aided segmentations implies that the FreeSurfer hippocampal subfield segmentation tool fails in epilepsy patients with HS. The segmentation algorithm is based upon a probability atlas derived from manual delineations of ex vivo and in vivo MRIs from ten healthy subjects, four subjects with Alzheimer's disease, and one subject with mild cognitive impairment [22]. We suspect that the FreeSurfer probability atlas is too rigid when setting priors for the hippocampal subfields in epilepsy patients and in particular in HS ILAE type 2 patients, where the subfield morphology is more unevenly distorted across the hippocampal subfields compared to healthy controls and patients with Alzheimer's disease [36].

4.3. Presurgical MRI as a Biomarker for Postsurgical Seizure Outcomes. In contrast to most published studies [5, 7, 37], we did not find a significant difference in seizure outcome one year after surgery in patients histopathologically diagnosed with HS compared to no-HS patients. The presurgical evaluation program varies among different epilepsy surgery centers, which will impact seizure outcome. In our centers, we acquire presurgical fluorodeoxyglucose positron emission tomography (FDG-PET) scans and intracranial EEG registration (ICR) in a relatively high proportion of MRI-negative patients or patients with discordant MRIs, seizure semiology, and EEG findings. Both FDG-PET [5, 37] and ICR [38, 39] are predictors of a positive surgical outcome. In our cohort, FDG-PET scans were acquired in 20 of 23 patients (87%) in the no-HS group who did not have an apparent lesion visible on MRI. Functional deficit zones concordant with the surgical resection site were present in 18 of these 20 patients. In 13/23 no-HS patients (57%), the epileptogenic zone was identified after ICR. In comparison, FDG-PET scans were acquired in 21/69 HS patients (45%) and ICR performed in 9/69 HS patients (13%). The good surgical outcomes of the no-HS patient group are most likely a result of the extensive presurgical evaluation program.

It is a dogma in epilepsy surgery that HS ILAE type is important for seizure freedom after hippocampectomy. In our study, no difference in seizure outcome was found between HS ILAE type 1 and 2 patients. However, the hypothesis that HS ILAE subtypes are predictive of seizure

freedom is supported by a limited number of studies: Blümcke et al. [40] found two of seven (29%) patients with neuronal loss restricted to the hilar region of hippocampus (\approx HS ILAE type 3) to achieve postsurgical seizure freedom, compared with 18 of 25 (72%) and six of nine (67%) of patients with neuronal loss similar to HS ILAE type 1 and type 2, respectively. In the studies by Thom et al. [41] and Stefan et al. [42], the patients with CA1 predominant HS (\approx HS ILAE type 2) had a poor seizure outcome. Calderon-Garcidueñas et al. [43] showed a significant reduction in long-term seizure freedom (Engel class 1a) only in a subgroup of HS ILAE type 1 patients with hypertrophic CA4 neurons. Thus, clinical significance of the failure of FreeSurfer to separate HS ILAE type 1 from HS ILAE type 2 appears limited. Nonetheless, future studies should include long-term postsurgical outcome assessments, as patients may have seizure relapse after the one-year follow-up period applied in our study.

5. Methodological Considerations

In this study, we provide strong clinical validation for using the HARNES-MRI protocol, computer-aided postprocessing in FreeSurfer, and a simple volume asymmetry ratio to separate patients diagnosed with HS from patients with other or normal pathology. However, it is important to emphasize that not all patients with a potential epileptogenic zone involving the hippocampus will benefit from computer-aided postprocessing of presurgical MRIs. According to Figure 1, 32/353 patients were excluded due to previous brain surgery, which hampers proper brain segmentation in FreeSurfer. FreeSurfer segmentation errors led to exclusion of 20/218 patients. Software for segmentation and methodology for correction of minor movement artefacts are likely to improve in the years to come, but for now, exclusion of 10% of the cohort is a large number. Five of 137 patients were excluded due to bilateral hippocampal pathology. This is probably an underestimation of the proportion of patients evaluated for epilepsy surgery with bilateral hippocampal pathology, since these patients are rarely offered epilepsy surgery. Using a volume asymmetry ratio as applied in our study precludes detection of subtle bilateral pathology, where the neuroradiological findings are scarce.

The right hippocampal volume has been demonstrated to be larger than the left hippocampal volume of healthy volunteers [44]. Although the difference in volume is small and large populations are needed to demonstrate a significant difference in volume with sufficient power, a subtle reduction in right hippocampal volume could in theory be outbalanced by an increase in hippocampal volume on the right side compared to the left side and influence our results. We found a significant difference in years of epilepsy and years of drug resistance between HS patients and no-HS patients, as well as a difference in mean age between the patients and the healthy control group of this study. Linear regression analysis found no correlation between age and VAR, and previous meta-analyses [44] on hippocampal asymmetry do not report changes in left-right asymmetry with increasing age. Finally, the results of this study are in-sample results, and validation in a new external dataset is warranted.

Data Availability

Given patients' sensitive information and General Data Protection Regulations (GDPR), the data that support the findings of this study is not publicly available. However, access to data (in anonymized form) will be granted from the corresponding author upon request but may require the completion of a formal data sharing agreement, in compliance with GDPR and Norwegian and Danish legislation.

Conflicts of Interest

None of the authors have any conflict of interest to disclose.

Acknowledgments

The project was supported by the Independent Research Fund Denmark | Medical Sciences (FSS) (grant ID: 7016-00151B), the Research Council of Rigshospitalet (grant ID: R181-A8114), the Lundbeck Foundation BrainDrugs (grant ID: R279-2018-1145), and Lundbeck Foundation (grant ID: R187-2015-2150). We thank the Norwegian Epilepsy Surgery group at the National Centre for Epilepsy and Rikshospitalet at Oslo University Hospital and the Danish Epilepsy Surgery group at the Copenhagen University Hospital-Rigshospitalet, and the Epilepsy Hospital Filadelfia for providing patient data. We thank Dr. Brice Ozenne for his valuable assistance with statistical analysis and Dr. Rune Markhus for assisting with retrieval of MRI data at Oslo University Hospital.

Supplementary Materials

MRI acquisition parameters. (*Supplementary Materials*)

References

- [1] A. Bernasconi, F. Cendes, W. H. Theodore et al., "Recommendations for the use of structural magnetic resonance imaging in the care of patients with epilepsy: a consensus report from the International League Against Epilepsy Neuroimaging Task Force," *Epilepsia*, vol. 60, no. 6, pp. 1054–1068, 2019.
- [2] I. Blümcke, "Neuropathology of focal epilepsies: a critical review," *Epilepsy and Behavior*, vol. 15, no. 1, pp. 34–39, 2009.
- [3] G. Shukla and A. N. Prasad, "Natural history of temporal lobe epilepsy: antecedents and progression," *Epilepsy Research and Treatment*, vol. 2012, Article ID 195073, 8 pages, 2012.
- [4] S. Wiebe and N. Jette, "Pharmacoresistance and the role of surgery in difficult to treat epilepsy," *Nature Reviews Neurology*, vol. 8, no. 12, pp. 669–677, 2012.
- [5] P. Ryvlin, J. H. Cross, and S. Rheims, "Epilepsy surgery in children and adults," *The Lancet Neurology*, vol. 13, no. 11, pp. 1114–1126, 2014.
- [6] S. West, S. J. Nolan, J. Cotton et al., "Surgery for epilepsy," *Cochrane Database of Systematic Reviews*, vol. 3, 2015.
- [7] S. Spencer and L. Huh, "Outcomes of epilepsy surgery in adults and children," *The Lancet Neurology*, vol. 7, no. 6, pp. 525–537, 2008.
- [8] I. Blümcke, M. Thom, E. Aronica et al., "International consensus classification of hippocampal sclerosis in temporal lobe epilepsy: a Task Force report from the ILAE Commission on

- Diagnostic Methods,” *Epilepsia*, vol. 54, no. 7, pp. 1315–1329, 2013.
- [9] M. Thom, “Review: hippocampal sclerosis in epilepsy: a neuropathology review,” *Neuropathology and Applied Neurobiology*, vol. 40, no. 5, pp. 520–543, 2014.
- [10] R. Coras, E. Pauli, J. Li et al., “Differential influence of hippocampal subfields to memory formation: insights from patients with temporal lobe epilepsy,” *Brain*, vol. 137, no. 7, pp. 1945–1957, 2014.
- [11] S. M. Comper, A. P. Jardim, J. T. Corso et al., “Impact of hippocampal subfield histopathology in episodic memory impairment in mesial temporal lobe epilepsy and hippocampal sclerosis,” *Epilepsy and Behavior*, vol. 75, no. 75, pp. 183–189, 2017.
- [12] F. Cendes, “Neuroimaging in investigation of patients with epilepsy,” *Continuum*, vol. 19, no. 3, pp. 623–642, 2013.
- [13] W. Van Paesschen, S. Sisodiya, A. Connelly et al., “Quantitative hippocampal MRI and intractable temporal lobe epilepsy,” *Neurology*, vol. 57, 11 SUPPL. 4, pp. S5–12, 2001.
- [14] M. Goubran, B. C. Bernhardt, D. Cantor-Rivera et al., “In vivo MRI signatures of hippocampal subfield pathology in intractable epilepsy,” *Human Brain Mapping*, vol. 37, no. 3, pp. 1103–1119, 2016.
- [15] S. B. Lee, Y. J. Cho, K. Jeon et al., “Diagnosis of hippocampal sclerosis in children: comparison of automated brain MRI volumetry and readers of varying experience,” *American Journal of Roentgenology*, vol. 217, no. 1, pp. 223–234, 2021.
- [16] G. Silva, C. Martins, N. Moreira da Silva et al., “Automated volumetry of hippocampus is useful to confirm unilateral mesial temporal sclerosis in patients with radiologically positive findings,” *The Neuroradiology Journal*, vol. 30, no. 4, pp. 318–323, 2017.
- [17] N. Farid, H. M. Girard, N. Kemmotsu et al., “Temporal lobe epilepsy: quantitative MR volumetry in detection of hippocampal atrophy,” *Radiology*, vol. 264, no. 2, pp. 542–550, 2012.
- [18] A. C. Coan, B. Kubota, F. P. G. Bergo, B. M. Campos, and F. Cendes, “3T MRI quantification of hippocampal volume and signal in mesial temporal lobe epilepsy improves detection of hippocampal sclerosis,” *American Journal of Neuroradiology*, vol. 35, no. 1, pp. 77–83, 2014.
- [19] D. Sone, N. Sato, N. Maikusa et al., “Automated subfield volumetric analysis of hippocampus in temporal lobe epilepsy using high-resolution T2-weighted MR imaging,” *NeuroImage: Clinical*, vol. 12, no. 12, pp. 57–64, 2016.
- [20] J. E. Peixoto-Santos, L. E. D. De Carvalho, L. Kandratavicius et al., “Manual hippocampal subfield segmentation using high-field MRI: impact of different subfields in hippocampal volume loss of temporal lobe epilepsy patients,” *Frontiers in Neurology*, vol. 9, 2018.
- [21] B. Fischl, “FreeSurfer,” *NeuroImage*, vol. 62, no. 2, pp. 774–781, 2012.
- [22] J. E. Iglesias, J. C. Augustinack, K. Nguyen et al., “A computational atlas of the hippocampal formation using ex vivo, ultra-high resolution MRI: application to adaptive segmentation of in vivo MRI,” *NeuroImage*, vol. 115, pp. 117–137, 2015.
- [23] K. Menzler, H. M. Hamer, P. Mross et al., “Validation of automatic MRI hippocampal subfield segmentation by histopathological evaluation in patients with temporal lobe epilepsy,” *Seizure*, vol. 87, pp. 94–102, 2021.
- [24] F. Riederer, R. Seiger, R. Lanzenberger et al., “Automated volumetry of hippocampal subfields in temporal lobe epilepsy,” *Epilepsy Research*, vol. 175, article 106692, 2021.
- [25] M. Mizutani, D. Sone, T. Sano et al., “Histopathological validation and clinical correlates of hippocampal subfield volumetry based on T2-weighted MRI in temporal lobe epilepsy with hippocampal sclerosis,” *Epilepsy Research*, vol. 177, article 106759, 2021.
- [26] G. Opheim, “Utilizing 7 Tesla MRI and Automated Segmentation – a New Era in the Presurgical Evaluation of Patients with Severe Epilepsy,” 2020, May 2023. <https://nru.dk/index.php/misc?catid=4&id=1044&m=0&task=download.send>.
- [27] G. M. Knudsen, P. S. Jensen, D. Erritzoe et al., “The Center for Integrated Molecular Brain Imaging (Cimbi) database,” *NeuroImage*, vol. 124, pp. 1213–1219, 2016.
- [28] H. G. Wieser, W. T. Blume, D. Fish et al., “Proposal for a new classification of outcome with respect to epileptic seizures following epilepsy surgery,” *Epilepsia*, vol. 42, no. 2, pp. 282–286, 2001.
- [29] B. Bechtold, *Violin Plots for Matlab*, Github Project, 2016.
- [30] J. M. Mettenberg, B. F. Branstetter, C. A. Wiley, P. Lee, and R. M. Richardson, “Improved detection of subtle mesial temporal sclerosis: validation of a commercially available software for automated segmentation of hippocampal volume,” *American Journal of Neuroradiology*, vol. 40, no. 3, pp. 440–445, 2019.
- [31] C. Hoppe, J. A. Witt, C. Helmstaedter, T. Gasser, H. Vatter, and C. E. Elger, “Laser interstitial thermotherapy (LiTT) in epilepsy surgery,” *Seizure*, vol. 48, pp. 45–52, 2017.
- [32] R. E. Gross, M. A. Stern, J. T. Willie et al., “Stereotactic laser amygdalohippocampotomy for mesial temporal lobe epilepsy,” *Annals of Neurology*, vol. 83, no. 3, pp. 575–587, 2018.
- [33] M. Quigg and C. Harden, “Minimally invasive techniques for epilepsy surgery: stereotactic radiosurgery and other technologies,” *Journal of Neurosurgery*, vol. 121, Suppl_2, pp. 232–240, 2014.
- [34] A. Labate, U. Aguglia, G. Tripepi et al., “Long-term outcome of mild mesial temporal lobe epilepsy,” *Neurology*, vol. 86, no. 20, pp. 1904–1910, 2016.
- [35] S. Wiebe, “Burden of intractable epilepsy,” *Advances in Neurology*, vol. 97, pp. 1–4, 2006.
- [36] N. M. Van Strien, M. Widerøe, W. D. J. Van De Berg, and H. B. M. Uylings, “Imaging hippocampal subregions with in vivo MRI: advances and limitations,” *Nature Reviews Neuroscience*, vol. 13, no. 1, p. 70, 2012.
- [37] A. L. Jones and G. D. Cascino, “Evidence on use of neuroimaging for surgical treatment of temporal lobe epilepsy,” *JAMA Neurology*, vol. 73, no. 4, pp. 464–470, 2016.
- [38] J. P. S. A. S. de Souza, J. Mullin, C. Wathen et al., “The usefulness of stereo-electroencephalography (SEEG) in the surgical management of focal epilepsy associated with “hidden” temporal pole encephalocele: a case report and literature review,” *Neurosurgical Review*, vol. 41, no. 1, pp. 347–354, 2018.
- [39] B. Garcia-Lorenzo, T. Del Pino-Sedeño, R. Rocamora, J. E. López, P. Serrano-Aguilar, and M. M. Trujillo-Martín, “Stereo-electroencephalography for refractory epileptic patients considered for surgery: systematic review, meta-analysis, and economic evaluation,” *Clinical Neurosurgery*, vol. 84, no. 2, pp. 326–338, 2019.
- [40] I. Blümcke, E. Pauli, H. Clusmann et al., “A new clinicopathological classification system for mesial temporal sclerosis,” *Acta Neuropathologica*, vol. 113, no. 3, pp. 235–244, 2007.
- [41] M. Thom, I. Liagkouras, K. J. Elliot et al., “Reliability of patterns of hippocampal sclerosis as predictors of postsurgical outcome,” *Epilepsia*, vol. 51, no. 9, pp. 1801–1808, 2010.

- [42] H. Stefan, M. Hildebrandt, F. Kerling et al., "Clinical prediction of postoperative seizure control: structural, functional findings and disease histories," *Journal of Neurology, Neurosurgery and Psychiatry*, vol. 80, no. 2, pp. 196–200, 2009.
- [43] A. L. Calderon-Garcidueñas, B. Mathon, P. Lévy et al., "New clinicopathological associations and histoprognostic markers in ILAE types of hippocampal sclerosis," *Brain Pathology*, vol. 28, no. 5, pp. 644–655, 2018.
- [44] O. Pedraza, D. Bowers, and R. Gilmore, "Asymmetry of the hippocampus and amygdala in MRI volumetric measurements of normal adults," *Journal of the International Neuropsychological Society*, vol. 10, no. 5, pp. 664–678, 2004.
- [45] P. Kwan, A. Arzimanoglou, A. T. Berg et al., "Definition of drug resistant epilepsy: consensus proposal by the ad hoc Task Force of the ILAE Commission on Therapeutic Strategies," *Epilepsia*, vol. 51, no. 6, pp. 1069–1077, 2010.